Kaempferol suppresses inflammation in mice suffering from both hyperuricemia and gouty arthritis through inhibiting NLRP3 inflammasome and NF-κB pathway

Yan Huang
Zhejiang Chinese Medical University
Cantao Li
Zhejiang Chinese Medical University
Wenjing Xu
Zhejiang Chinese Medical University
Fenfen Li
Zhejiang Chinese Medical University
Changyu Xu
Zhejiang Chinese Medical University
Chenxi Wu
Zhejiang Chinese Medical University
Yihuan Wang
Zhejiang Chinese Medical University
Xiaoxi Zhang
Academy of Chinese Medical Sciences, Zhejiang Chinese Medical University
Daozong Xia (xdz_zjtcm@hotmail.com)
Zhejiang Chinese Medical University

Research Article

Keywords: hyperuricemia, gouty arthritis, kaempferol, renal transporters, NLRP3 inflammasome, NF-κB pathway

Posted Date: May 19th, 2023

DOI: https://doi.org/10.21203/rs.3.rs-2946547/v1

Abstract

The co-occurrence of hyperuricemia and gouty arthritis is common in patients, yet a suitable animal model for this condition is lacking. In present study, a mice model combined hyperuricemia and gouty arthritis was established. Kaempferol, a flavonoid compound with anti-inflammatory and urate-lowering properties, was administered to mice in different dosages (25, 50, and 100 mg/kg). The levels of uric acid, creatinine, blood urea nitrogen and xanthine oxidase activity were measured, then kidney and joint ankle tissues were examined for pathological changes. The expressions of renal transporters, oxidative stress and inflammatory cytokines were detected. Furthermore, the anti-inflammatory mechanism of kaempferol was verified from NOD-like receptor protein 3 (NLRP3) inflammasome and nuclear factor kappa B (NF-κB) pathway. The results of histological analyses showed that kaempferol ameliorated the glomerular and renal tubular lesions and ankle arthritis inflammatory infiltration caused by hyperuricemia combined with gouty arthritis. Additionally, treatment with kaempferol effectively alleviated oxidative stress and decreased the levels of pro-inflammatory cytokines. The research confirmed that kidney and joint inflammation in hyperuricemia combined with gouty arthritis mice were alleviated by kaempferol via suppressing NLRP3 inflammasome and NF-κB pathway.

INTRODUCTION

Hyperuricemia is a metabolic disease caused by a disorder of purine metabolism and an imbalance of uric acid (UA) formation and secretion, which is often accompanied by elevated the levels of pro-inflammatory factors and oxidative stress [1,2]. It is a major predisposing factor for gout and attacks more likely to occur in those with high serum UA [3]. With the continuous improvement of people's living conditions, the intake of high-protein, high-fructose, and high-purine foods have increased. This has led to a rising incidence of hyperuricemia and its complication, gouty arthritis, in the population. The age of disease onset is also tending to be younger. NOD-like receptor protein 3 (NLRP3) inflammasome plays a crucial role in the pathogenesis of inflammation. The activation of it is widely believed to occur through two sequential steps, referred to as priming and assembly. The priming step is triggered by pattern recognition receptors such as Toll-like receptors (TLRs), which activates the signaling pathway mediated by nuclear factor kappa B (NF-κB) [4,5]. In the activation step, various stimuli, such as extracellular ATP, mitochondrial DNA, and pathogen-related components, trigger the assembly of NLRP3 inflammasome complexes. This leads to the recruitment and activation of Caspase-1, which cleaves pro-interleukin (IL-1β) and pro-IL-18 to generate their mature forms. The release of mature IL-1β and IL-18 triggers inflammatory responses [6–8]. Several studies have demonstrated that regulating NLRP3 inflammasome activation is a promising strategy for the treatment of hyperuricemia and gouty arthritis. For instance, phloretin was shown to attenuate hyperuricemia-induced chronic renal dysfunction via inhibiting NLRP3 inflammasome activation [9]. In addition, gallic acid was reported to suppress gouty arthritis by inhibiting NLRP3 inflammasome activation and pyroptosis [10]. Thus, inhibiting inflammation through regulating NLRP3 inflammasome serves as a potential strategy for the treatment of hyperuricemia and gouty arthritis.

Currently, two primary types of animal models for gout are recognized: hyperuricemia models and gouty arthritis models. Hyperuricemia models have been established through the oral administration of a mixture of adenine and potassium oxonate (PO), or through a combination of peritoneal injection of PO and intragastric administration of hypoxanthine [9,11]. Gouty arthritis models, on the other hand, have been successfully established in previous studies by injecting with monosodium urate (MSU) into ankle joints [12,13]. However, given that hyperuricemia and gouty arthritis often occur simultaneously in patients, the development of a combined animal model for these conditions is currently lacking.

The majority of clinical therapeutic drugs currently available for the treatment of hyperuricemia and gouty arthritis exhibit significant side-effects. Allopurinol, a prototypical xanthine oxidase (XOD) inhibitor, is effective in only a fraction of patients with hyperuricemia, and is associated with the risk of renal toxicity and hypersensitivity reactions [14]. Colchicine, commonly prescribed to relieve gouty arthritis symptoms, may have a stimulating effect on the gastrointestinal tract, leading to gastrointestinal bleeding [15,16]. Benzbromarone, used for treating both hyperuricemia and gouty arthritis, is prescribed with caution due to its hepatotoxicity [17]. Therefore, there is an urgent need to identify a safe and effective approach for preventing and treating the combined manifestation of hyperuricemia and gouty arthritis.

In recent years, natural products-based drugs have been considered a novel therapeutic strategy for preventing and treating inflammatory diseases. Among the various plant constituents in natural products, flavonoids, which are present in many herbal medicines and plant-based foods, are considered the most active compounds [18]. Kaempferol is a widely occurring dietary bioflavonoid found in various fruits, vegetables, Chinese herbal medicines and other natural plants, which has a range of pharmacological benefits, including antioxidant and anti-inflammatory properties [19–21]. In particular, kaempferol has been found to exhibit reversible competitive inhibition of XOD activity, making it a potentially useful biological agent for treating hyperuricemia [22].

Taken together, we wonder if kaempferol was capable of protecting against hyperuricemia and the subsequent gouty arthritis. In present study, a mice model combined hyperuricemia and gouty arthritis was established. Serum, urine and liver biochemical analysis, as well as articular and renal histological assessment, were then performed to evaluate treating hyperuricemia and anti-gout arthritis effects of kaempferol. Additionally, superoxide dismutase (SOD), glutathione (GSH) and glutathione peroxidase (GSH-Px) activities, malondialdehyde (MDA) level, and the levels of inflammatory factors IL-1β, IL-6 and tumor necrosis factor (TNF)-α were also determined. To further explore the mechanisms, the effect of kaempferol on renal transporters, NLRP3 inflammasome and NF-κB pathway were investigated through Western blotting analysis.

MATERIALS DNA METHODS

Materials and reagents

Kaempferol (purity > 95%, Lot: J09GS153993) was purchased from Shanghai yuanye Biotechnology Co., Ltd. (Shanghai, China). Colchicine tablets (Lot: 20210202) were purchased from PIDI Pharmaceutical Co., Ltd. (Guangdong, China). Benzbromarone tablets (Lot: 0062008023) were purchased from HEC Pharmaceutical Co., Ltd. (Yichang, China). PO (Lot: STBH8632), xanthine (Lot: SLBM5210V) and MSU (Lot: BC8R7559) were purchased from Sigma-Aldrich (St. Louis, MO, US). XOD (Lot: 20211104), creatinine (CRE, Lot: 20211102), blood urea nitrogen (BUN, Lot: 20211102), SOD (Lot: 20211103), GSH (Lot: 20211102), GSH-Px (Lot: 20211103) and MDA (Lot: 20211104) texting kits were provided by Nanjing Jiancheng Bioengineering Institute (Nanjing, China). IL-1β (Lot: 1161759622) and TNF-α (Lot: 241171031026) ELISA kits were purchased from Boster Biological Technology Co., Ltd. (Wuhan, China). IL-6 ELISA kit (Lot: MM-0163M1) was purchased from MEIMIAN (Shanghai, China). Bicinchoninic Acid (BCA) Protein Assay Kit was purchased from Beyotime Institute of Biotechnology (Shanghai, China). Primary antibodies against NLRP3 (Lot: 5), ASC (Lot: 2), Caspase-1 (Lot: 4), p-IKKα (Lot: 21), IKKα (Lot: 5), p-p65 (Lot: 17), p65 (Lot: 16), p-IκBα (Lot: 18), IκBα (Lot: 11), ATP-binding cassette transporter G2 (ABCG2, Lot: 2), β-actin (Lot: 18) and anti-rabbit IgG HRP-linked antibodies (Lot: 29) were supplied by Cell Signaling Technology (Boston, MA, USA). Primary antibodies against organic anion transporter 1 (OAT1, Lot: GR3202420-5) and organic anion transporters 2 (OCT2, Lot: GR153338-2) were produced by Abcam (Cambridge, MA, USA). Primary antibodies against glucose transporter 9 (GLUT9, Lot: 67530-1-IG) was purchased from Proteintech (Wuhan, China). Goat anti-mouse IgG HRP-conjugated secondary antibody (Lot: L3032) was purchased from Signaling Antibody (College Park, MD, USA).

Animals

Male C57BL/6 mice (6-week-old) weighting about 20 g, were purchased from Shanghai SLAC Laboratory Animals Co., Ltd., and housed at Zhejiang Chinese Medical University Laboratory Animal Research Center (Permit Number: SYXK 2018-0012). All experimental procedures followed the Guide for the Care and Use of Laboratory Animals (National Institutes of Health (NIH), Bethesda, MD, United States) and approved by Animal Ethical and Welfare Committee of Zhejiang Chinese Medical University (Ethical Approval Number: 20180813-01).

Establishment of a model combined hyperuricemia and gouty arthritis

Mice were randomly divided into seven groups: control group, model group, three different concentrations of kaempferol groups (25, 50 and 100 mg/kg), and two positive control groups administrated with colchicine (1 mg/kg) and benzbromarone (10 mg/kg). Hyperuricemia model was induced by intraperitoneal injection of PO and xanthine both at the concentration of 280 mg/kg. Mice in control group were intraperitoneally injected with the same amount of saline solution. In other groups, mice were established with hyperuricemia model and treated with colchicine, benzbromarone and kaempferol by intragastric administration once per day for 14 days. On day 13, mice were intra-articular injected with 25 μL (1.25 mg) MSU suspension into bilateral ankle joints 1 h after intragastric administration except that in control group. Mice in control group were injected with the same amount of saline solution at the same time. Individual urine samples were collected using metabolism cages on the last day of the study. Then

all mice were sacrificed. Blood samples were collected and incubated at 37°C for 1 h and then centrifuged at 3,500 rpm for 15 min at 4°C to separate serum. Liver, kidney and ankle tissues were also collected and stored at − 80°C for further measurements.

Measurement of ankle joint swelling

A horizontal line was drawn at 0.5 cm on the ankle of with a fadeless marker as a unified standard for measuring the volume of toes before injection. The toe volume was measured before and 2, 4, 6, 20 and 24 h after model establishment with a toe volume measuring device [12,13]. The obtained data were calculated according to the following formula. The process of measurements was conducted by an experimenter blind to treatment allocation.

$$\text{Swelling index (\%)} = \frac{\text{Vafter injection - Vbefore injection}}{\text{Vbefore injection}} \times 100\%$$

Serum, urine and liver biochemical analysis

Liver tissues were mixed with normal saline to prepare 10% (*w/v*) homogenate and centrifuged at 3,000 rpm for 10 min at 4°C to separate supernatant. BUN and CRE concentrations in serum and urine, as well as hepatic XOD activity were measured according to manufacturer instructions. The UA concentrations in serum and urine were measured using the phosphotungstic acid method [23]. Glomerular filtration rate (GFR) was estimated by calculating CRE clearance, which was done by using 24 h urine volume and CRE concentrations in both serum and urine via the following formula [24,25].

$$\text{GFR} = \frac{\text{urine CRE} \times \text{V24 h}}{1440 \times \text{serum CRE}}$$

Antioxidant activity

Kidney tissues were mixed with normal saline to prepare 10% (*w/v*) homogenate and centrifuged at 3,000 rpm for 10 min at 4°C to separate supernatant. Activities of SOD, GSH, GSH-Px and MDA level were detected by using commercial detection kits.

ELISA assay

Ankle and kidney tissues were mixed with normal saline to prepare 10% (*w/v*) homogenate and centrifuged at 3,000 rpm for 10 min at 4°C to separate supernatant. ELISA was employed to determine the concentrations of articular IL-1β, IL-6 and TNF-α and renal IL-1β, and measurements were carried out according to the manufacturer's protocols.

Histopathological examination

Ankle and kidney tissues were both fixed using 4% paraformaldehyde at room temperature for 24 h (ankle tissues were decalcified in ethylenediaminetetraacetic acid (EDTA) after fixation). Then kidney and ankle tissues were embedded in paraffin, and subsequently were cut into 4 μm sections. Both tissue sections

were stained with Hematoxylin and eosin (H&E) for histopathological examination according to the standard protocol.

Western blotting

Proteins were extracted from ankle and kidney tissues using RIPA buffer containing 1% phosphatase inhibitor and protease inhibitor, and concentrations were determined by using a BCA Protein Assay Kit. Proteins were denatured by heating in a metal bath for 10 min. Then equal aliquots of proteins were separated on 10% SDS-PAGE, and transferred onto polyvinylidene fluoride (PVDF) membranes, followed by blocking with 5% (*w/v*) non-fat milk dissolved in TBST for 1 h at room temperature. The membranes were then incubated with the primary antibodies over night at 4°C and secondary antibodies for 1 h at room temperature. Protein bands on the membranes were visualized through enhanced chemiluminescence (ECL) reagents. The densitometric analysis of the bands was quantified using Image J software tools.

Statistical analysis

Statistical analysis was performed using a GraphPad Prism 8.0. One-way analysis of variance (ANOVA) followed by Dunnett's multiple comparisons test was used to evaluate the differences across multiple groups. All data were expressed as mean ± SEM and $p < 0.05$ was considered to represent statistical significance.

RESULTS

Kaempferol alleviated ankle joint swelling in mice

To investigate the effects of kaempferol, the degree of ankle joint swelling was measured and observed. Marked ankle joint swelling could be seen 2 h after MSU injection compared to control group, reaching the maximum at 6 h (Fig. 1B, Table 1). As shown in Fig. 1A, after kaempferol treatment, the gouty symptoms were relieved, indicating kaempferol could alleviated ankle joint swelling.

Table 1
Measurement of swelling index of mice ankle joints (%)

Group	Dose	2 h	4 h	6 h	20 h	24 h
Control	—	23.92 ± 0.41	34.58 ± 0.71	31.41 ± 1.12	20.09 ± 0.93	16.93 ± 0.82
Model	50 mg/mL	30.27 ± 1.20$^{\#}$	55.90 ± 1.73$^{\#\#}$	64.71 ± 0.66$^{\#\#}$	53.19 ± 0.95$^{\#\#}$	47.61 ± 1.11$^{\#\#}$
Kaempferol	25 mg/kg	27.60 ± 2.93	48.01 ± 1.55**	58.74 ± 1.16**	44.13 ± 1.72**	35.68 ± 1.51**
	50 mg/kg	26.95 ± 1.19	42.69 ± 0.81**	52.76 ± 1.05**	39.36 ± 1.88**	29.87 ± 0.81**
	100 mg/kg	25.53 ± 0.93	44.06 ± 2.08**	53.25 ± 1.25**	35.00 ± 2.59**	29.56 ± 2.53**
Colchicine	1 mg/kg	26.36 ± 1.08	43.54 ± 0.32**	49.62 ± 1.37**	32.35 ± 1.82**	25.88 ± 1.25**
Benzbromarone	10 mg/kg	29.86 ± 0.95	46.98 ± 0.87**	53.58 ± 1.07**	34.10 ± 0.77**	30.35 ± 1.24**

Data are shown as mean ± SEM (n = 10). $^{\#}p < 0.05$, $^{\#\#}p < 0.01$ vs. control group. $^{**}p < 0.01$ vs. model group.

Kaempferol suppressed inflammatory cell infiltration and inhibited cytokine productions in mice ankle joints

Histological analyses of mice ankle joints showed that fewer inflammatory cell infiltration in control group, while abundant inflammatory cell infiltration in model group. Kaempferol treatment resulted in a significant reduction in the influx of inflammatory cells. (Fig. 2A). Since MSU has been reported to induce the expressions of pro-inflammatory cytokines (IL-1β, IL-6, and TNF-α), leading to the aggravation of inflammatory reaction [26,27], we further investigated the levels of articular IL-1β, IL-6 and TNF-α in mice. As shown in Fig. 2B-D, significantly elevated the levels of IL-1β, IL-6 and TNF-α were found after MSU injection compared to that of control group ($p < 0.01$). Kaempferol treatment significantly reversed the elevations of IL-1β, IL-6 and TNF-α compared to model group ($p < 0.01$). All data showed that kaempferol could reduce the inflammatory cell infiltration and inhibited cytokine productions in mice ankle joints.

Kaempferol promoted UA excretion and reduced hepatic XOD activity in mice

As shown in Fig. 3A, B, there were significant reduction in the level of urine UA and CRE in model group when comparing to those in control group ($p < 0.01$). Administration with kaempferol at 25, 50 and 100

mg/kg both effectively increased the levels of urine UA and CRE compared to those of model group ($p < 0.01$). However, the levels of serum UA as well as indicators of renal function involving serum CRE and BUN changed in the opposite direction (Fig. 3C-E). GFR is one of the important indexes to evaluate renal function. As shown in Fig. 3F, GFR in model group was dramatically lower than that in control group ($p < 0.01$), while kaempferol treatment increased GFR significantly ($p < 0.01$). In addition, the key enzyme XOD is closely related to the production of UA [28,29]. Hepatic XOD activity in model mice was evidently higher than that in control mice ($p < 0.01$), while administration with kaempferol decreased hepatic XOD activity compared to model mice ($p < 0.01$).

Kaempferol modulated renal urate transport-associated proteins in mice

The expressions of renal urate transport-associated proteins were quantitatively detected by Western blotting. Results in Fig. 4 showed that the protein expressions of ABCG2, OCT2 and OAT1 in model group were significantly down-regulated compared to control group, while the protein expression of GLUT9 in model group was significantly up-regulated compared to control group. Kaempferol could effectively reverse the abnormal protein expressions of ABCG2, OAT1, OCT2 and GLUT9 in kidneys.

Kaempferol alleviated renal oxidative stress in mice

The activities of antioxidative enzymes including SOD, GSH and GSH-Px and the level of MDA, an oxidative stress marker, were also measured (Fig. 5A-D). Compared with control group, obviously decreased activities of SOD, GSH and GSH-Px and an increased the level of MDA were observed in model group ($p < 0.01$). However, we observed that kaempferol reversed the reduction of SOD, GSH and GSH-Px activities and the elevation of MDA level, especially for high-dose kaempferol treatment (100 mg/kg). These data demonstrated that kaempferol alleviated kidney oxidative stress.

Kaempferol improved histopathological changes and inhibited cytokine production in kidneys of mice

H&E-staining showed that kidney tissue morphology was normal in control mice, while model mice exhibited several characterized histologic alterations of renal injury, including inconspicuous boundary between adjacent proximal tubule cells, glomerular atrophy and tubular swelling. However, treatment with kaempferol could reverse the above effects (Fig. 6A). Additionally, as shown in Fig. 6B, it not difficult to find an obvious production of IL-1β in model mice in comparison to control group ($p < 0.01$). Nevertheless, kaempferol treatment could dose-dependently inhibited the production of IL-1β ($p < 0.01$).

Kaempferol suppressed activation of NLRP3 inflammasome and NF-κB pathway in ankle joints

In order to further confirm the mechanisms of kaempferol in mice ankle joints, NLRP3 inflammasome and NF-κB pathway associated proteins were conducted (Fig. 7A, B). NLRP3, Caspase-1, ASC, p-IKKα/IKKα, p-p65/p65 and p-IκBα/IκBα protein expressions in model mice were significantly increased in comparison

to control group. After kaempferol administration, the protein expressions of those were decreased compared to model group.

Kaempferol improved kidney inflammation by suppressing NLRP3 inflammasome activation in mice

As mentioned above, kaempferol had ability to reduce the level of inflammatory cytokine IL-1β in kidneys (Fig. 6B), and IL-1β is one of the downstream products of NLRP3 inflammatory pathway [30]. Depending on these foundations, we further investigated the effect of kaempferol on NLRP3 inflammasome. As shown in Fig. 8, the protein expressions of NLRP3 and ASC were significantly increased in kidneys of model group compared to control group. Kaempferol treatment reduced the protein expressions of NLRP3 and ASC, suggesting that kaempferol suppressed the activation of NLRP3 inflammasome to improve kidney inflammation.

DISCUSSION

UA is a weak acid and its ionized form present in the body is urate at physiologic pH [31]. The pathological threshold of hyperuricemia is defined as 6.8 mg/dL (the in vitro solubility limit of MSU) [1,32]. When the level of serum UA is higher than the normal threshold, MSU crystals deposition begins to occur in tissues. Nevertheless, when the deposition of MSU crystals occurs in articular cartilage, synovial sacs and other tissues, it will cause inflammation with concomitant swelling and pain, which is called gouty arthritis. It can be said that hyperuricemia is the most important risk factor for gouty arthritis. The clinical picture of gout is divided into four stages: asymptomatic hyperuricemia, acute gouty arthritis, intercritical period, and chronic tophaceous gout [31]. Several studies disclosed MSU deposits in a proportion of asymptomatic hyperuricemia patients [33,34]. There are many separate animal models have been widely developed to investigate the causal mechanisms for hyperuricemia or gout but do not yet reliably and simultaneously simulate hyperuricemia and its complication gouty arthritis that occurs in humans. For protection, it is necessary to prevent UA from the formation of MSU crystals, which is effective in the treatment of gout. A combined hyperuricemia and gouty arthritis animal model will be in line with the population in the transition stage from asymptomatic hyperuricemia to acute gouty arthritis in clinical practice, which is a relatively new application model. Therefore, this combined model has more obvious research value and significance. In present study, marked ankle joint swelling and abundant inflammatory cell infiltration could be seen in ankle joint of model group. We also observed significant elevation of serum UA, CRE and BUN levels and reduction of urine UA and CRE levels in model mice. As our data indicated, we successfully induced a model combined hyperuricemia and gouty arthritis in mice by combination of intraperitoneal injection of PO and xanthine and intra-articular injection of MSU crystals [12,13,35,36].

Following kaempferol treatment, the photographs and H&E-staining of mice ankle joints demonstrated similar changes that kaempferol significantly alleviated MSU crystals-induced joint inflammation (ankle swelling and inflammatory cell infiltration), controlling the onset of gouty arthritis in mice. Also,

kaempferol could also increase the excretion of UA and CRE in the kidney, which might ameliorate hyperuricemia and renal dysfunction, as well as caused the levels of serum UA, CRE and BUN tend to normal. Higher XOD activity can lead to excessive synthesis of UA [37,38]. Besides, treatment with kaempferol could significantly inhibit hepatic XOD activity, suggesting that the effect of kaempferol on reducing UA production might be due to the inhibition of XOD activity. Moreover, kaempferol showed a potential protective effect on renal injury by suppressing oxidative stress through activating the SOD, GSH and GSH-Px and reducing MDA. In short, the remarkable improvement in biochemical parameters and histopathologic changes were observed after kaempferol treatment, indicating the urate-lowering and decreasing inflammatory responses effects of kaempferol.

The transport and excretion of UA are complicated procedures which are related with various renal transporters, including GLUT9, ABCG2, OAT1, OCT2 and so on [39,40]. Specifically speaking, GLUT9 is expressed on basolateral membranes and is capable of transporting UA from renal tubules into the circulation [9]. ABCG2 is a high-capacity urate exporter and the reduced extra-renal UA excretion resulting from ABCG2 dysfunctional variants is a common cause of hyperuricemia [41,42]. OAT1 mediates urate secretion from the blood into the tubular lumen [42,43]. Elevated expression of OAT1 has been observed to promote the excretion of UA into urine, thereby leading to a decrease in the concentration of UA in serum. A decrease in the expression or malfunction of OAT1 has been shown to significantly elevate the likelihood of developing hyperuricemia [44,45]. Besides, OCT2 that exists on the basolateral membrane of renal tubules, plays the pivotal roles in absorption, distribution and excretion of hydrophilic organic cations [46]. According to previous studies, empagliflozin treatment was attributed to UA excretion promotion through up-regulating ABCG2 expression in KK-Ay mice with hyperuricemia [11]. Similarly, saponins induced the decrease of serum UA and increase the excretion of urine UA through up-regulating the GLUT9 expression level and down-regulating the OAT1 expression level in chronic hyperuricemia rats [47]. Astaxanthin also promoted UA excretion by down-regulating the protein expressions of GLUT9, as well as up-regulating the protein expressions of OAT1 and ABCG2 [48]. Consistent with previous findings, we found that kaempferol could effectively reverse the abnormal protein expressions of GLUT9, ABCG2, OAT1 and OCT2 in kidneys of mice. In brief, the anti-hyperuricemia effect, at least in part, is achieved by regulating renal transporter expressions [49–51]. Dysregulation of renal transporters can lead to excessive accumulation of UA in the body, which may activate inflammation.

As for inflammation, it is characterized by coordinated activation of various signaling pathways. NLRP3 interacts with the bridging molecule ASC to increase the expression of Caspase-1, which plays an important role in maturing IL-1β and IL-18 expressions [52]. The NLRP3 inflammasome activation triggers kidney and joint inflammatory response along with the up-regulation of IL-1β and IL-18 [53,54]. Moreover, NF-κB is produced by homologous or heterodimerization of Rel family proteins, mainly in the form of p50 and p65 subunits. Under normal conditions, NF-κB in the cytoplasm remains inactive and binds to the inhibitory protein IκB. Once stimulated, IκB kinase (IKK) is involved in the phosphorylation of IκBα, which then mediates the phosphorylation of NF-κB p65 [55]. In this study, the levels of inflammatory cytokines in model group were significantly higher than those in control group, and NLRP3 inflammasome and NF-κB pathway were activated, as evidenced by the up-regulated protein expressions of NLRP3, Caspase-1,

ASC, p-IKKα/IKKα, p-p65/p65 and p-IκBα/IκBα. However, kaempferol treatment significantly reversed the elevations of inflammatory cytokines. Notably, different dosages of kaempferol could reduce the expression of the above proteins to varying degrees, which indicated that kaempferol might exert anti-inflammatory effects, including reducing inflammatory cytokine release and inflammatory cell infiltration into the lesion site, mediated by the suppression of NLRP3 inflammasome and NF-κB pathways. Previous studies also have shown that MAPK, TLR4 and AR/NOX2 signaling pathways are involved in the antioxidant or anti-inflammatory process of kaempferol [56,57]. Overall, the findings suggest that kaempferol possesses anti-inflammatory effects, potentially mediated through multiple signaling pathways.

It cannot be ignored that the development potential of dietary flavonoids might be limited due to their low solubility, absorption, and rapid metabolism. To address these limitations, various strategies have been developed to deliver poorly water-soluble flavonoids, including the use of an absorption enhancer, structural transformation (e.g., prodrugs, glycosylation), and pharmaceutical technologies (e.g., carrier complexes, cocrystals). Nanotechnology has shown promise in enhancing the bioavailability and systemic absorption of certain chemical compounds. It has been reported that kaempferol can be encapsulated using a coating of nanoparticles of poly (lactic acid-co-glycolic acid) and polyethylene oxide-poly propylene oxide-polyethylene oxide, which was effective in reducing cancer cell viability as compared to alone kaempferol [58]. In the study of Ilk, kaempferol was loaded into lecithin/chitosan nanoparticles to make antifungal activity more effective compared to pure kaempferol [59]. Moreover, kaempferol loaded chitosan nanoparticles enhanced the anti-quorum sensing activity [60]. However, whether the anti-inflammatory effects of kaempferol could be enhanced by these approaches remains to be studied.

CONCLUSION

Our research findings provide evidence that the administration of kaempferol demonstrates urate-lowering and anti-inflammatory effects in a combined hyperuricemia and gouty arthritis mice model. Kaempferol effectively ameliorated inflammation in the kidneys and ankles of mice by reducing inflammatory cell infiltration and decreasing the production of inflammatory cytokines. Furthermore, kaempferol reversed the abnormal expression of renal transporters, leading to an increased excretion of UA. In conclusion, our study demonstrates that kaempferol exerts anti-inflammatory effects in mice with hyperuricemia and gouty arthritis through the inhibition of NLRP3 inflammasome and NF-κB pathway, highlighting its potential as a therapeutic agent for the treatment of these conditions.

Declarations

ACKNOWLEDGEMENTS

The authors gratefully acknowledged the support from the Public Platform of Pharmaceutical and Medical Research Center, Academy of Chinese Medical Science, Zhejiang Chinese Medical University.

AUTHOR CONTRIBUTION

Daozong Xia initiated the research idea, performed experimental design and got funding support. Yan Huang, Cantao Li and Wenjing Xu performed most of the experiments. Changyu Xu, Chenxi Wu and Yihuan Wang collected and analyzed the data. Yan Huang wrote the first draft of manuscript. Fenfen Li and Xiaoxi Zhang reviewed and edited the manuscript. All authors read and approved the final manuscript.

FUNDING

This work was supported by National Natural Science Foundation of China (82074085, 82204726), Zhejiang Provincial Natural Science Foundation (LQ22H280008), Opening Project of Zhejiang Provincial Preponderant and Characteristic Subject of Key University (Traditional Chinese Pharmacology) of Zhejiang Chinese Medical University (ZYAOXZD2019002), and Postgraduate Scientific Research Fund of Zhejiang Chinese Medical University (2021YKJ25, 2022YKJ20).

DATA AVAILABILITY

The data and materials that support the findings of this study are available from the corresponding author upon reasonable request.

Ethics Approval The animal study protocol was approved by the Animal Ethical and Welfare Committee of Zhejiang Chinese Medical University (Ethical Approval Number: 20180813-01).

Consent to Participate Not applicable.

Consent for Publication All the authors have read the manuscript and agreed to submit the paper to the journal.

Conflict of Interest The authors declare no competing interests.

References

1. Kim, I.Y., K.D. Han, D.H. Kim, Y. Eun, H.S. Cha, E.M. Koh, et al. 2019. Women with metabolic syndrome and general obesity are at a higher risk for significant hyperuricemia compared to men. *Journal of Clinical Medicine* 8 (6). https://doi.org/10.3390/jcm8060837
2. Taguchi, K., S. Hamamoto, A. Okada, R. Unno, H. Kamisawa, T. Naiki, et al. 2017. Genome-wide gene expression profiling of randall's plaques in calcium oxalate stone formers. *Journal of the American Society of Nephrology* 28 (1): 333-347. https://doi.org/10.1681/asn.2015111271
3. Schlesinger, N., J.M. Norquist and D.J. Watson. 2009. Serum urate during acute gout. *Journal of Rheumatology* 36 (6): 1287-1289. https://doi.org/10.3899/jrheum.080938
4. Bauernfeind, F.G., G. Horvath, A. Stutz, E.S. Alnemri, K. MacDonald, D. Speert, et al. 2009. Cutting edge: Nf-kappab activating pattern recognition and cytokine receptors license nlrp3 inflammasome

activation by regulating nlrp3 expression. *Journal of Immunology* 183 (2): 787-791. https://doi.org/10.4049/jimmunol.0901363

5. Swanson, K.V., M. Deng and J.P. Ting. 2019. The nlrp3 inflammasome: Molecular activation and regulation to therapeutics. *Nature Reviews Immunology* 19 (8): 477-489. https://doi.org/10.1038/s41577-019-0165-0
6. Broz, P., J. von Moltke, J.W. Jones, R.E. Vance and D.M. Monack. 2010. Differential requirement for caspase-1 autoproteolysis in pathogen-induced cell death and cytokine processing. *Cell Host & Microbe* 8 (6): 471-483. https://doi.org/10.1016/j.chom.2010.11.007
7. Latz, E., T.S. Xiao and A. Stutz. 2013. Activation and regulation of the inflammasomes. *Nature Reviews Immunology* 13 (6): 397-411. https://doi.org/10.1038/nri3452
8. Renaudin, F., L. Orliaguet, F. Castelli, F. Fenaille, A. Prignon, F. Alzaid, et al. 2020. Gout and pseudo-gout-related crystals promote glut1-mediated glycolysis that governs nlrp3 and interleukin-1β activation on macrophages. *Annals of the Rheumatic Diseases* 79 (11): 1506-1514. https://doi.org/10.1136/annrheumdis-2020-217342
9. Cui, D., S. Liu, M. Tang, Y. Lu, M. Zhao, R. Mao, et al. 2020. Phloretin ameliorates hyperuricemia-induced chronic renal dysfunction through inhibiting nlrp3 inflammasome and uric acid reabsorption. *Phytomedicine* 66: 153111. https://doi.org/10.1016/j.phymed.2019.153111
10. Lin, Y., T. Luo, A. Weng, X. Huang, Y. Yao, Z. Fu, et al. 2020. Gallic acid alleviates gouty arthritis by inhibiting nlrp3 inflammasome activation and pyroptosis through enhancing nrf2 signaling. *Frontiers in Immunology* 11: 580593. https://doi.org/10.3389/fimmu.2020.580593
11. Lu, Y.H., Y.P. Chang, T. Li, F. Han, C.J. Li, X.Y. Li, et al. 2020. Empagliflozin attenuates hyperuricemia by upregulation of abcg2 via ampk/akt/creb signaling pathway in type 2 diabetic mice. *International Journal of Biological Sciences* 16 (3): 529-542. https://doi.org/10.7150/ijbs.33007
12. Wu, C., F. Li, X. Zhang, W. Xu, Y. Wang, Y. Yao, et al. 2022. (-)-epicatechin ameliorates monosodium urate-induced acute gouty arthritis through inhibiting nlrp3 inflammasome and the nf-κb signaling pathway. *Frontiers in Pharmacology* 13: 799552. https://doi.org/10.3389/fphar.2022.799552
13. Xu, W., F. Li, X. Zhang, C. Wu, Y. Wang, Y. Yao, et al. 2022. The protective effects of neoastilbin on monosodium urate stimulated thp-1-derived macrophages and gouty arthritis in mice through nf-κb and nlrp3 inflammasome pathways. *Molecules* 27 (11). https://doi.org/10.3390/molecules27113477
14. Pacher, P., A. Nivorozhkin and C. Szabó. 2006. Therapeutic effects of xanthine oxidase inhibitors: Renaissance half a century after the discovery of allopurinol. *Pharmacological Reviews* 58 (1): 87-114. https://doi.org/10.1124/pr.58.1.6
15. Schlesinger, N. 2017. The safety of treatment options available for gout. *Expert Opinion on Drug Safety* 16 (4): 429-436. https://doi.org/10.1080/14740338.2017.1284199
16. Shi, Y., H. Cai, Z. Niu, J. Li, G. Pan, H. Tian, et al. 2021. Acute oral colchicine caused gastric mucosal injury and disturbance of associated microbiota in mice. *Toxicology* 461: 152908. https://doi.org/10.1016/j.tox.2021.152908

17. Azevedo, V.F., I.A. Kos, A.B. Vargas-Santos, G. da Rocha Castelar Pinheiro and E. Dos Santos Paiva. 2019. Benzbromarone in the treatment of gout. *Advances in Rheumatology* 59 (1): 37. https://doi.org/10.1186/s42358-019-0080-x
18. Yi, Y.S. 2018. Regulatory roles of flavonoids on inflammasome activation during inflammatory responses. *Molecular Nutrition & Food Research* 62 (13): e1800147. https://doi.org/10.1002/mnfr.201800147
19. Matei, I. and M. Hillebrand. 2010. Interaction of kaempferol with human serum albumin: A fluorescence and circular dichroism study. *Journal of Pharmaceutical and Biomedical Analysis* 51 (3): 768-773. https://doi.org/10.1016/j.jpba.2009.09.037
20. Tsai, M.S., Y.H. Wang, Y.Y. Lai, H.K. Tsou, G.G. Liou, J.L. Ko, et al. 2018. Kaempferol protects against propacetamol-induced acute liver injury through cyp2e1 inactivation, ugt1a1 activation, and attenuation of oxidative stress, inflammation and apoptosis in mice. *Toxicology Letters* 290: 97-109. https://doi.org/10.1016/j.toxlet.2018.03.024
21. Choung, W.J., S.H. Hwang, D.S. Ko, S.B. Kim, S.H. Kim, S.H. Jeon, et al. 2017. Enzymatic synthesis of a novel kaempferol-3-o-β-d-glucopyranosyl-(1→4)-o-α-d-glucopyranoside using cyclodextrin glucanotransferase and its inhibitory effects on aldose reductase, inflammation, and oxidative stress. *Journal of Agricultural and Food Chemistry* 65 (13): 2760-2767. https://doi.org/10.1021/acs.jafc.7b00501
22. Wang, Y., G. Zhang, J. Pan and D. Gong. 2015. Novel insights into the inhibitory mechanism of kaempferol on xanthine oxidase. *Journal of Agricultural and Food Chemistry* 63 (2): 526-534. https://doi.org/10.1021/jf505584m
23. Niu, Y., W. Lu, L. Gao, H. Lin, X. Liu and L. Li. 2012. Reducing effect of mangiferin on serum uric acid levels in mice. *Pharmaceutical Biology* 50 (9): 1177-1182. https://doi.org/10.3109/13880209.2012.663763
24. Inker, L.A. and S. Titan. 2021. Measurement and estimation of gfr for use in clinical practice: Core curriculum 2021. *American Journal of Kidney Diseases* 78 (5): 736-749. https://doi.org/10.1053/j.ajkd.2021.04.016
25. Yin, C., B. Liu, P. Wang, X. Li, Y. Li, X. Zheng, et al. 2020. Eucalyptol alleviates inflammation and pain responses in a mouse model of gout arthritis. *British Journal of Pharmacology* 177 (9): 2042-2057. https://doi.org/10.1111/bph.14967
26. Caution, K., N. Young, F. Robledo-Avila, K. Krause, A. Abu Khweek, K. Hamilton, et al. 2019. Caspase-11 mediates neutrophil chemotaxis and extracellular trap formation during acute gouty arthritis through alteration of cofilin phosphorylation. *Frontiers in Immunology* 10: 2519. https://doi.org/10.3389/fimmu.2019.02519
27. Oosterhuis, N.R., R. Fernandes, N. Maicas, S.E. Bae, J. Pombo, H. Gremmels, et al. 2017. Extravascular renal denervation ameliorates juvenile hypertension and renal damage resulting from experimental hyperleptinemia in rats. *Journal of Hypertension* 35 (12): 2537-2547. https://doi.org/10.1097/hjh.0000000000001472

28. Isaka, Y., Y. Takabatake, A. Takahashi, T. Saitoh and T. Yoshimori. 2016. Hyperuricemia-induced inflammasome and kidney diseases. *Nephrology Dialysis Transplantation* 31 (6): 890-896. https://doi.org/10.1093/ndt/gfv024
29. Si, Y., J.W. Park, S. Jung, G.S. Hwang, E. Goh and H.J. Lee. 2018. Layer-by-layer electrochemical biosensors configuring xanthine oxidase and carbon nanotubes/graphene complexes for hypoxanthine and uric acid in human serum solutions. *Biosensors & Bioelectronics* 121: 265-271. https://doi.org/10.1016/j.bios.2018.08.074
30. Ruiz, P.A., B. Morón, H.M. Becker, S. Lang, K. Atrott, M.R. Spalinger, et al. 2017. Titanium dioxide nanoparticles exacerbate dss-induced colitis: Role of the nlrp3 inflammasome. *Gut* 66 (7): 1216-1224. https://doi.org/10.1136/gutjnl-2015-310297
31. Ragab, G., M. Elshahaly and T. Bardin. 2017. Gout: An old disease in new perspective - a review. *Journal of Advanced Research* 8 (5): 495-511. https://doi.org/10.1016/j.jare.2017.04.008
32. Dalbeth, N., T.R. Merriman and L.K. Stamp. 2016. Gout. *Lancet* 388 (10055): 2039-2052. https://doi.org/10.1016/s0140-6736(16)00346-9
33. Bardin, T. and P. Richette. 2014. Definition of hyperuricemia and gouty conditions. *Current Opinion in Rheumatology* 26 (2): 186-191. https://doi.org/10.1097/bor.0000000000000028
34. Chen-Xu, M., C. Yokose, S.K. Rai, M.H. Pillinger and H.K. Choi. 2019. Contemporary prevalence of gout and hyperuricemia in the united states and decadal trends: The national health and nutrition examination survey, 2007-2016. *Arthritis & Rheumatology* 71 (6): 991-999. https://doi.org/10.1002/art.40807
35. Chen, J., L. Xu, L. Jiang, Y. Wu, L. Wei, X. Wu, et al. 2021. Sonneratia apetala seed oil attenuates potassium oxonate/hypoxanthine-induced hyperuricemia and renal injury in mice. *Food & Function* 12 (19): 9416-9431. https://doi.org/10.1039/d1fo01830b
36. Yong, T., M. Zhang, D. Chen, O. Shuai, S. Chen, J. Su, et al. 2016. Actions of water extract from cordyceps militaris in hyperuricemic mice induced by potassium oxonate combined with hypoxanthine. *Journal of Ethnopharmacology* 194: 403-411. https://doi.org/10.1016/j.jep.2016.10.001
37. Adachi, S.I., K. Sasaki, S. Kondo, W. Komatsu, F. Yoshizawa, H. Isoda, et al. 2020. Antihyperuricemic effect of urolithin a in cultured hepatocytes and model mice. *Molecules* 25 (21). https://doi.org/10.3390/molecules25215136
38. Zhao, X., J.X. Zhu, S.F. Mo, Y. Pan and L.D. Kong. 2006. Effects of cassia oil on serum and hepatic uric acid levels in oxonate-induced mice and xanthine dehydrogenase and xanthine oxidase activities in mouse liver. *Journal of Ethnopharmacology* 103 (3): 357-365. https://doi.org/10.1016/j.jep.2005.08.040
39. Maiuolo, J., F. Oppedisano, S. Gratteri, C. Muscoli and V. Mollace. 2016. Regulation of uric acid metabolism and excretion. *International Journal of Cardiology* 213: 8-14. https://doi.org/10.1016/j.ijcard.2015.08.109

40. Wang, Z., T. Cui, X. Ci, F. Zhao, Y. Sun, Y. Li, et al. 2019. The effect of polymorphism of uric acid transporters on uric acid transport. *Journal of Nephrology* 32 (2): 177-187. https://doi.org/10.1007/s40620-018-0546-7
41. Toyoda, Y., A. Mančíková, V. Krylov, K. Morimoto, K. Pavelcová, J. Bohatá, et al. 2019. Functional characterization of clinically-relevant rare variants in abcg2 identified in a gout and hyperuricemia cohort. *Cells* 8 (4). https://doi.org/10.3390/cells8040363
42. Wang, S., Y. Fang, X. Yu, L. Guo, X. Zhang and D. Xia. 2019. The flavonoid-rich fraction from rhizomes of smilax glabra roxb. Ameliorates renal oxidative stress and inflammation in uric acid nephropathy rats through promoting uric acid excretion. *Biomedicine & Pharmacotherapy* 111: 162-168. https://doi.org/10.1016/j.biopha.2018.12.050
43. Su, J., Y. Wei, M. Liu, T. Liu, J. Li, Y. Ji, et al. 2014. Anti-hyperuricemic and nephroprotective effects of rhizoma dioscoreae septemlobae extracts and its main component dioscin via regulation of moat1, murat1 and moct2 in hypertensive mice. *Archives of Pharmacal Research* 37 (10): 1336-1344. https://doi.org/10.1007/s12272-014-0413-6
44. Liu, H.C., N. Jamshidi, Y. Chen, S.A. Eraly, S.Y. Cho, V. Bhatnagar, et al. 2016. An organic anion transporter 1 (oat1)-centered metabolic network. *Journal of Biological Chemistry* 291 (37): 19474-19486. https://doi.org/10.1074/jbc.M116.745216
45. Yong, T., S. Chen, Y. Xie, D. Chen, J. Su, O. Shuai, et al. 2018. Hypouricemic effects of armillaria mellea on hyperuricemic mice regulated through oat1 and cnt2. *American Journal of Chinese Medicine* 46 (3): 585-599. https://doi.org/10.1142/s0192415x18500301
46. Aoki, M., T. Terada, M. Kajiwara, K. Ogasawara, I. Ikai, O. Ogawa, et al. 2008. Kidney-specific expression of human organic cation transporter 2 (oct2/slc22a2) is regulated by DNA methylation. *American Journal of Physiology-Renal Physiology* 295 (1): F165-170. https://doi.org/10.1152/ajprenal.90257.2008
47. Zhu, L., Y. Dong, S. Na, R. Han, C. Wei and G. Chen. 2017. Saponins extracted from dioscorea collettii rhizomes regulate the expression of urate transporters in chronic hyperuricemia rats. *Biomedicine & Pharmacotherapy* 93: 88-94. https://doi.org/10.1016/j.biopha.2017.06.022
48. Le, Y., X. Zhou, J. Zheng, F. Yu, Y. Tang, Z. Yang, et al. 2020. Anti-hyperuricemic effects of astaxanthin by regulating xanthine oxidase, adenosine deaminase and urate transporters in rats. *Marine Drugs* 18 (12). https://doi.org/10.3390/md18120610
49. Becker, M.A., P.A. Simkin and L.B. Sorensen. 2014. Urate transporters: Transforming the face of hyperuricemia and gout. *Journal of Rheumatology* 41 (10): 1910-1912. https://doi.org/10.3899/jrheum.141019
50. Eckenstaler, R. and R.A. Benndorf. 2021. The role of abcg2 in the pathogenesis of primary hyperuricemia and gout-an update. *International Journal of Molecular Sciences* 22 (13). https://doi.org/10.3390/ijms22136678
51. Lin, G., Q. Yu, L. Xu, Z. Huang, L. Mai, L. Jiang, et al. 2021. Berberrubine attenuates potassium oxonate- and hypoxanthine-induced hyperuricemia by regulating urate transporters and jak2/stat3

signaling pathway. *European Journal of Pharmacology* 912: 174592. https://doi.org/10.1016/j.ejphar.2021.174592

52. Duewell, P., H. Kono, K.J. Rayner, C.M. Sirois, G. Vladimer, F.G. Bauernfeind, et al. 2010. Nlrp3 inflammasomes are required for atherogenesis and activated by cholesterol crystals. *Nature* 464 (7293): 1357-1361. https://doi.org/10.1038/nature08938
53. Chen, Z., H. Zhong, J. Wei, S. Lin, Z. Zong, F. Gong, et al. 2019. Inhibition of nrf2/ho-1 signaling leads to increased activation of the nlrp3 inflammasome in osteoarthritis. *Arthritis Research & Therapy* 21 (1): 300. https://doi.org/10.1186/s13075-019-2085-6
54. Vilaysane, A., J. Chun, M.E. Seamone, W. Wang, R. Chin, S. Hirota, et al. 2010. The nlrp3 inflammasome promotes renal inflammation and contributes to ckd. *Journal of the American Society of Nephrology* 21 (10): 1732-1744. https://doi.org/10.1681/asn.2010020143
55. Mitchell, J.P. and R.J. Carmody. 2018. Nf-κb and the transcriptional control of inflammation. *International Review of Cell and Molecular Biology* 335: 41-84. https://doi.org/10.1016/bs.ircmb.2017.07.007
56. Yuan, P., X. Sun, X. Liu, G. Hutterer, K. Pummer, B. Hager, et al. 2021. Kaempferol alleviates calcium oxalate crystal-induced renal injury and crystal deposition via regulation of the ar/nox2 signaling pathway. *Phytomedicine* 86: 153555. https://doi.org/10.1016/j.phymed.2021.153555
57. Zhong, X., L. Zhang, Y. Li, P. Li, J. Li and G. Cheng. 2018. Kaempferol alleviates ox-ldl-induced apoptosis by up-regulation of mir-26a-5p via inhibiting tlr4/nf-κb pathway in human endothelial cells. *Biomedicine & Pharmacotherapy* 108: 1783-1789. https://doi.org/10.1016/j.biopha.2018.09.175
58. Luo, H., B. Jiang, B. Li, Z. Li, B.H. Jiang and Y.C. Chen. 2012. Kaempferol nanoparticles achieve strong and selective inhibition of ovarian cancer cell viability. *International Journal of Nanomedicine* 7: 3951-3959. https://doi.org/10.2147/ijn.S33670
59. Ilk, S., N. Saglam and M. Özgen. 2017. Kaempferol loaded lecithin/chitosan nanoparticles: Preparation, characterization, and their potential applications as a sustainable antifungal agent. *Artificial Cells Nanomedicine and Biotechnology* 45 (5): 907-916. https://doi.org/10.1080/21691401.2016.1192040
60. Ilk, S., N. Sağlam, M. Özgen and F. Korkusuz. 2017. Chitosan nanoparticles enhances the anti-quorum sensing activity of kaempferol. *International Journal of Biological Macromolecules* 94 (Pt A): 653-662. https://doi.org/10.1016/j.ijbiomac.2016.10.068

Figures

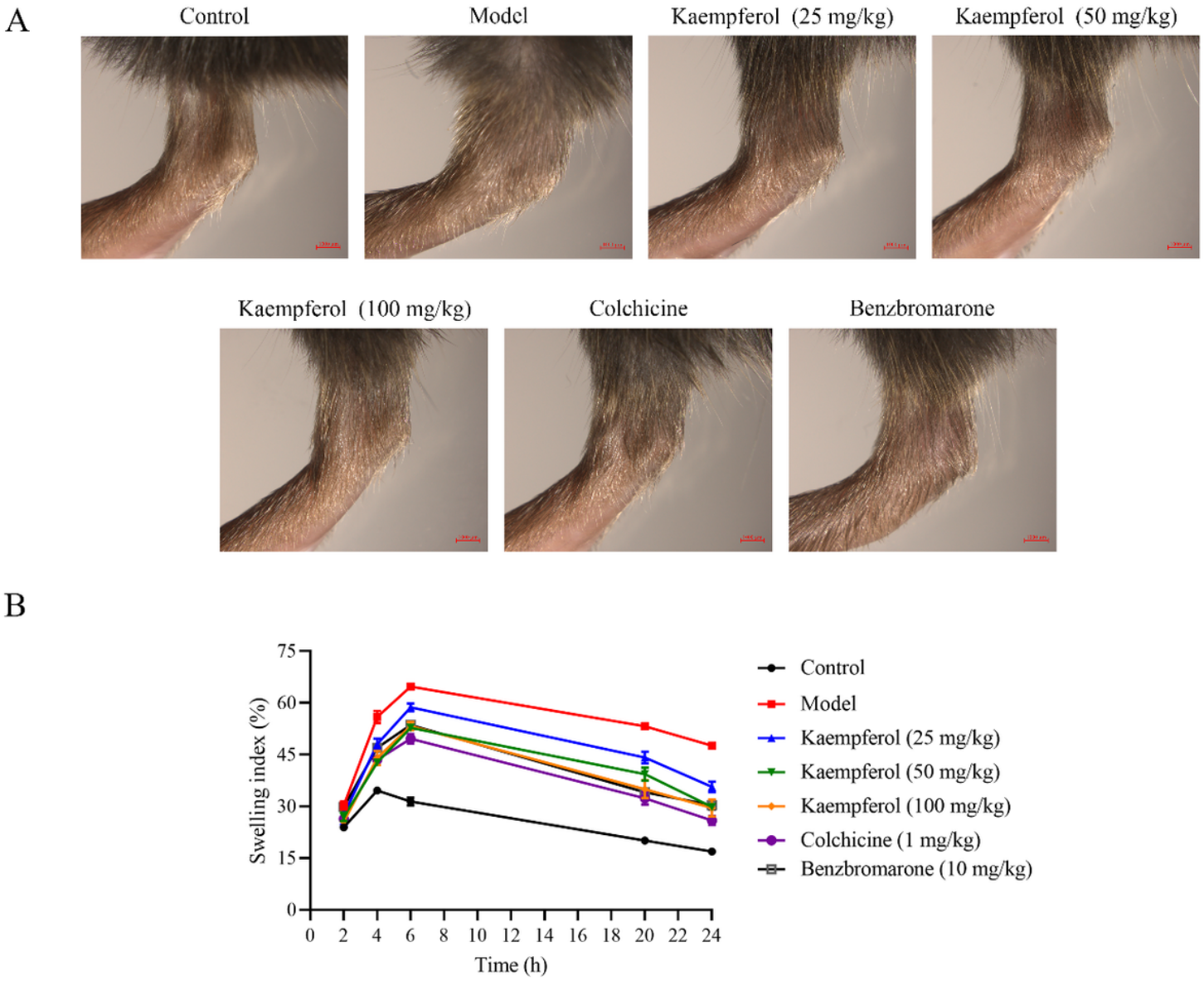

Figure 1

Effect of kaempferol on ankle joint swelling in mice: (**A**) Representative photographs of ankle joint swelling in mice 24 h after MSU injection; (**B**) The tendency of swelling index.

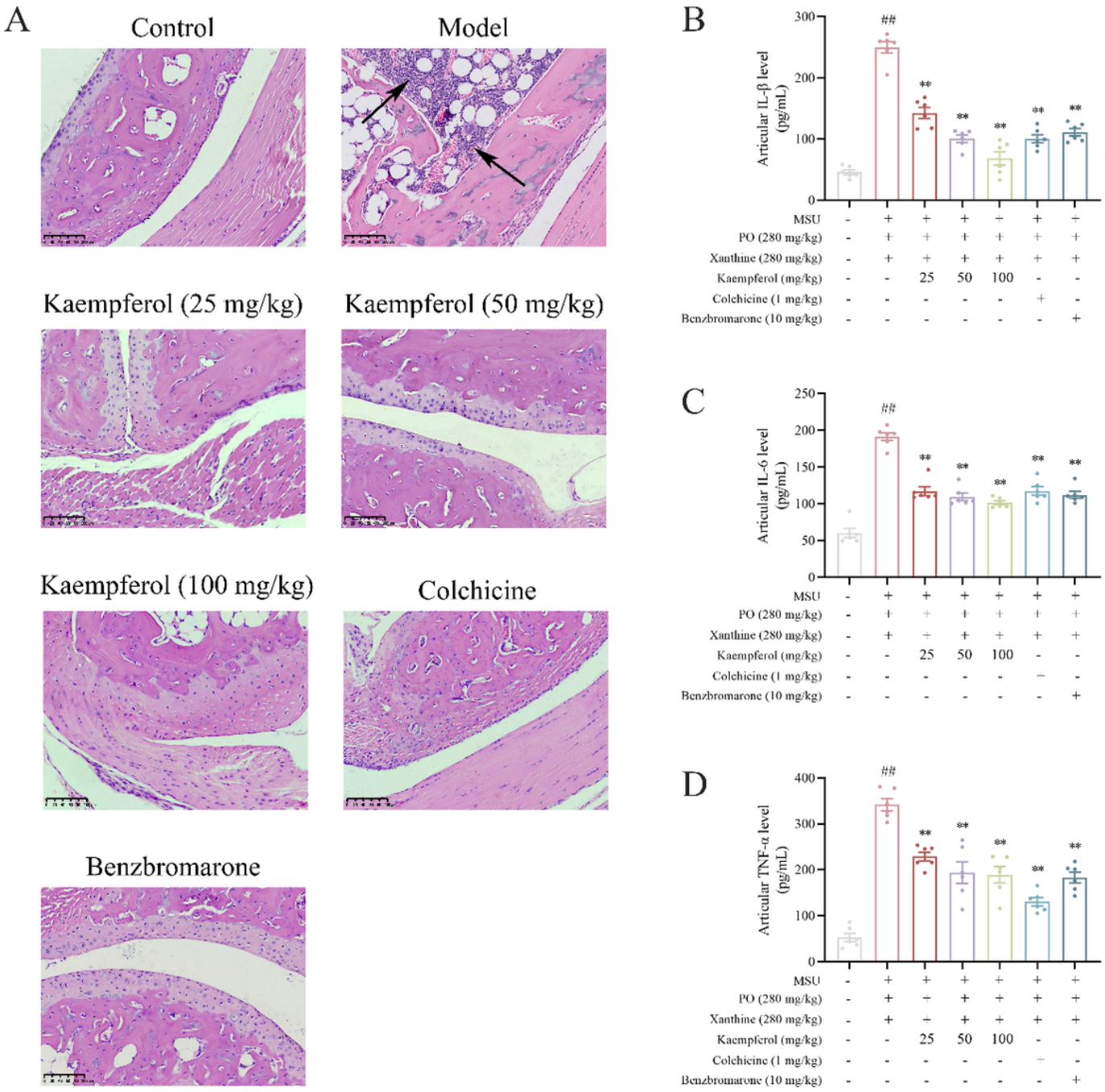

Figure 2

Representative H&E-staining showing in mice ankle joints (**A**). The arrows indicate the infiltrating inflammatory cells; Effect of kaempferol on the levels of IL-Iβ (**B**), IL-6 (**C**) and TNF-α (**D**) in mice ankle joints. Data are shown as mean ± SEM (n=6). $^{\#\#}p < 0.01$ vs. control group. $^{**}p < 0.01$ vs. model group.

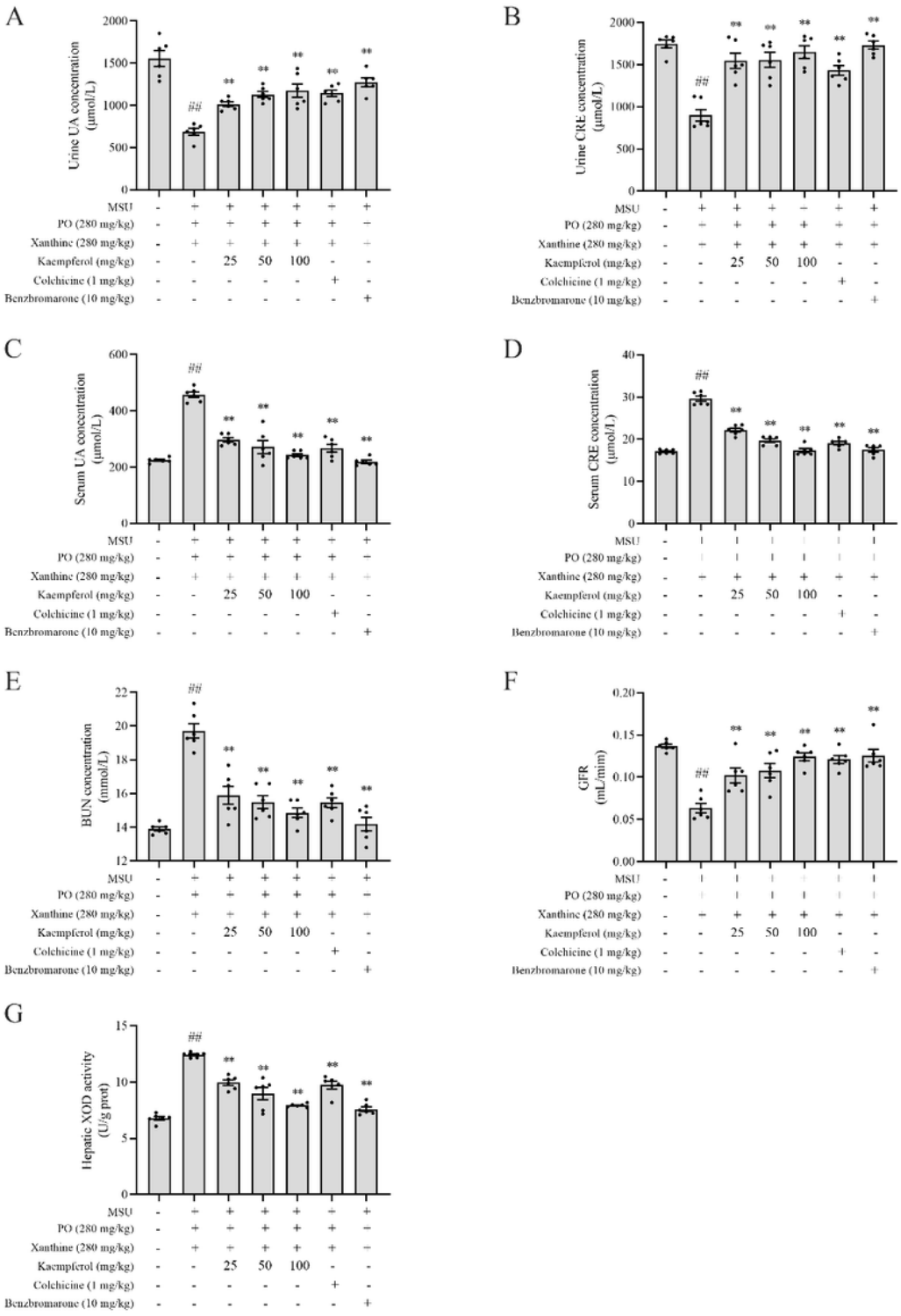

Figure 3

Effect of kaempferol on urine UA concentration (**A**), urine CRE concentration (**B**), serum UA concentration (**C**), serum CRE concentration (**D**), BUN concentration (**E**), glomerular filtration rate (**F**) and hepatic XOD activity (**G**) in mice. Data are shown as mean ± SEM (n=6). $^{\#\#}p < 0.01$ vs. control group. $^{**}p < 0.01$ vs. model group.

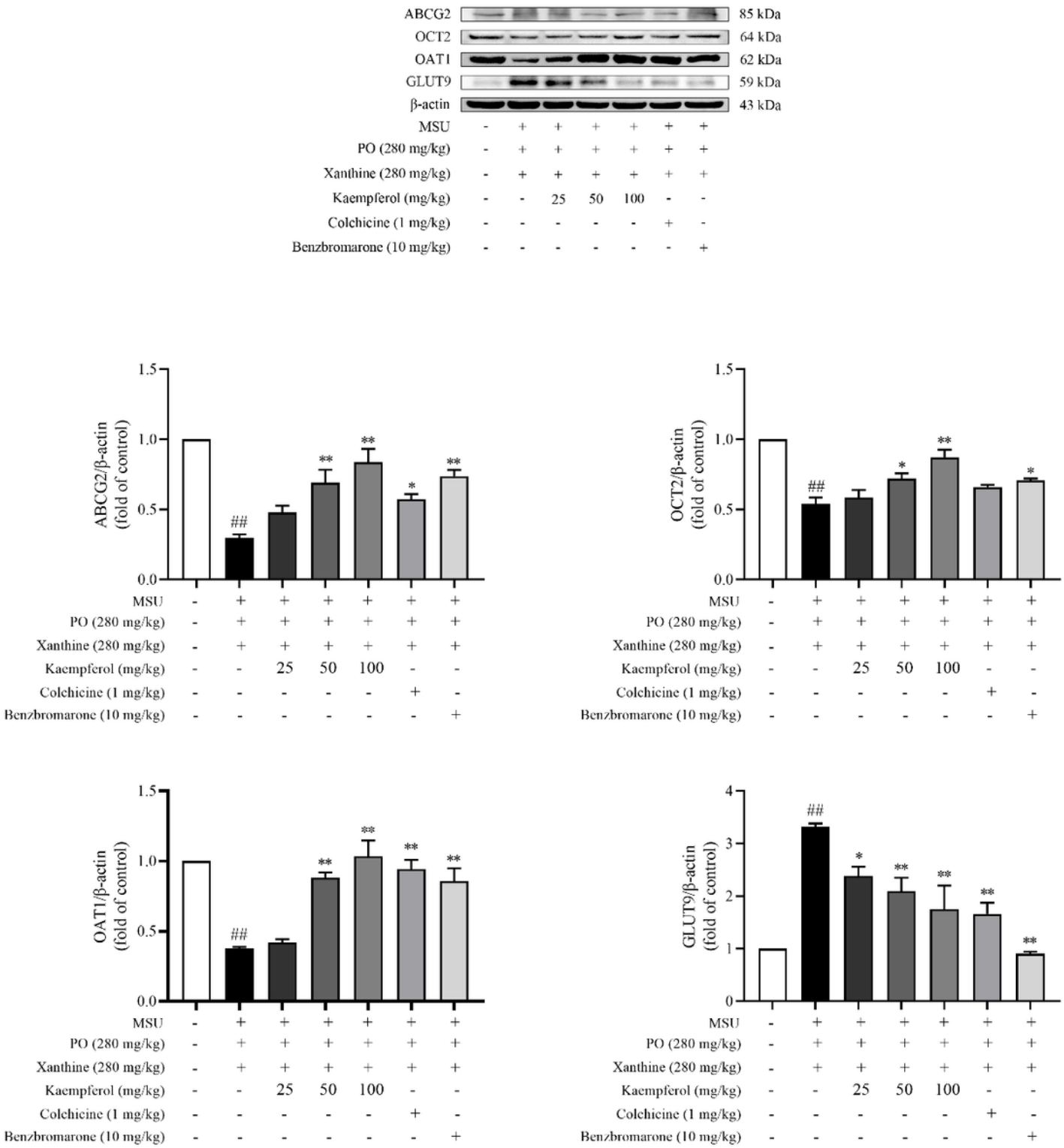

Figure 4

Effect of kaempferol on the expressions of renal urate transport-associated proteins in mice. Data are shown as mean ± SEM (n=3). $^{\#\#}p < 0.01$ vs. control group. $^{*}p < 0.05$, $^{**}p < 0.01$ vs. model group.

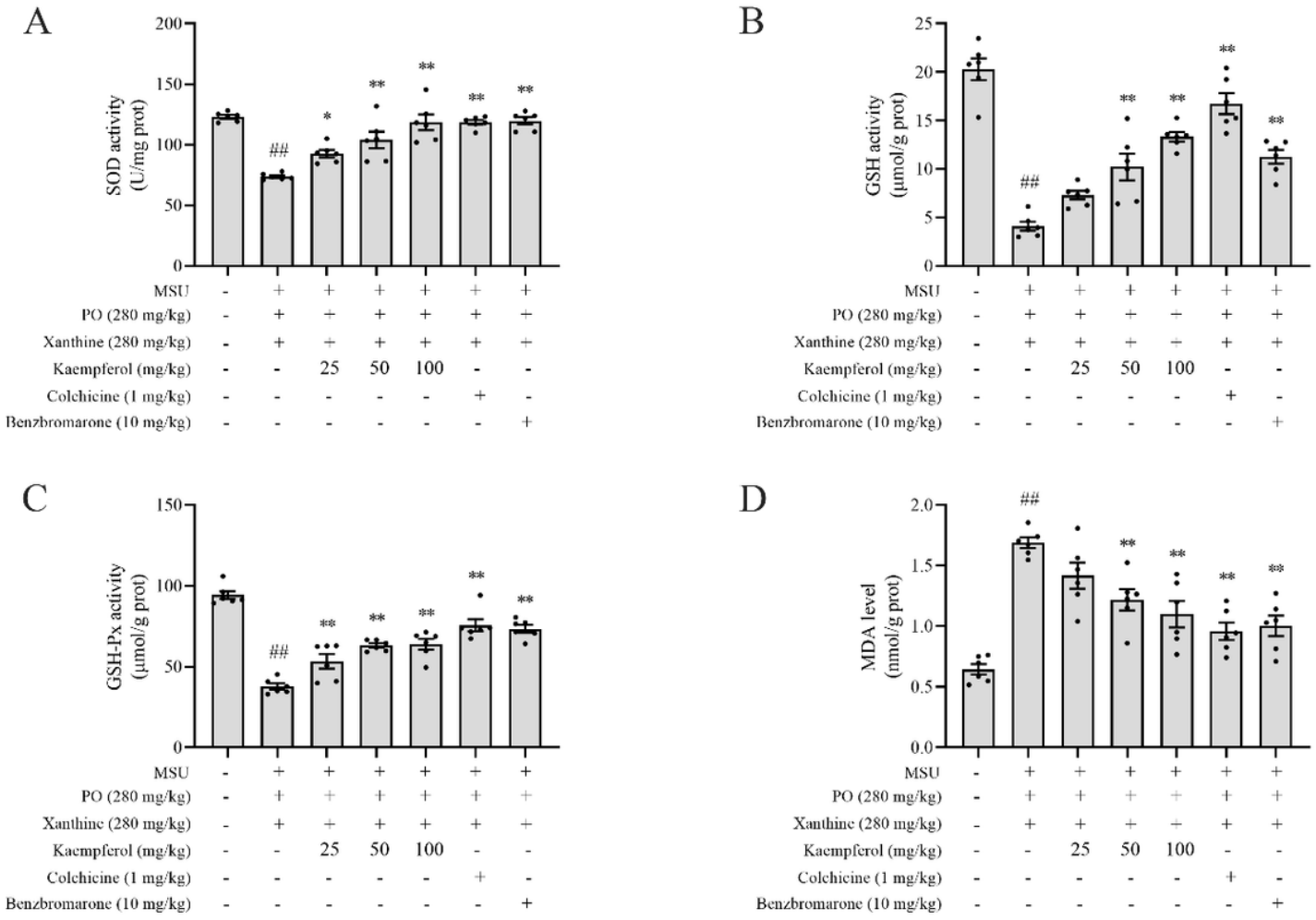

Figure 5

Effect of kaempferol on SOD activity (**A**), GSH activity (**B**), GSH-Px activity (**C**) and MDA level (**D**) in mice kidneys. Data are shown as mean ± SEM (n=6). $^{\#\#}p < 0.01$ vs. control group. $^{*}p < 0.05$, $^{**}p < 0.01$ vs. model group.

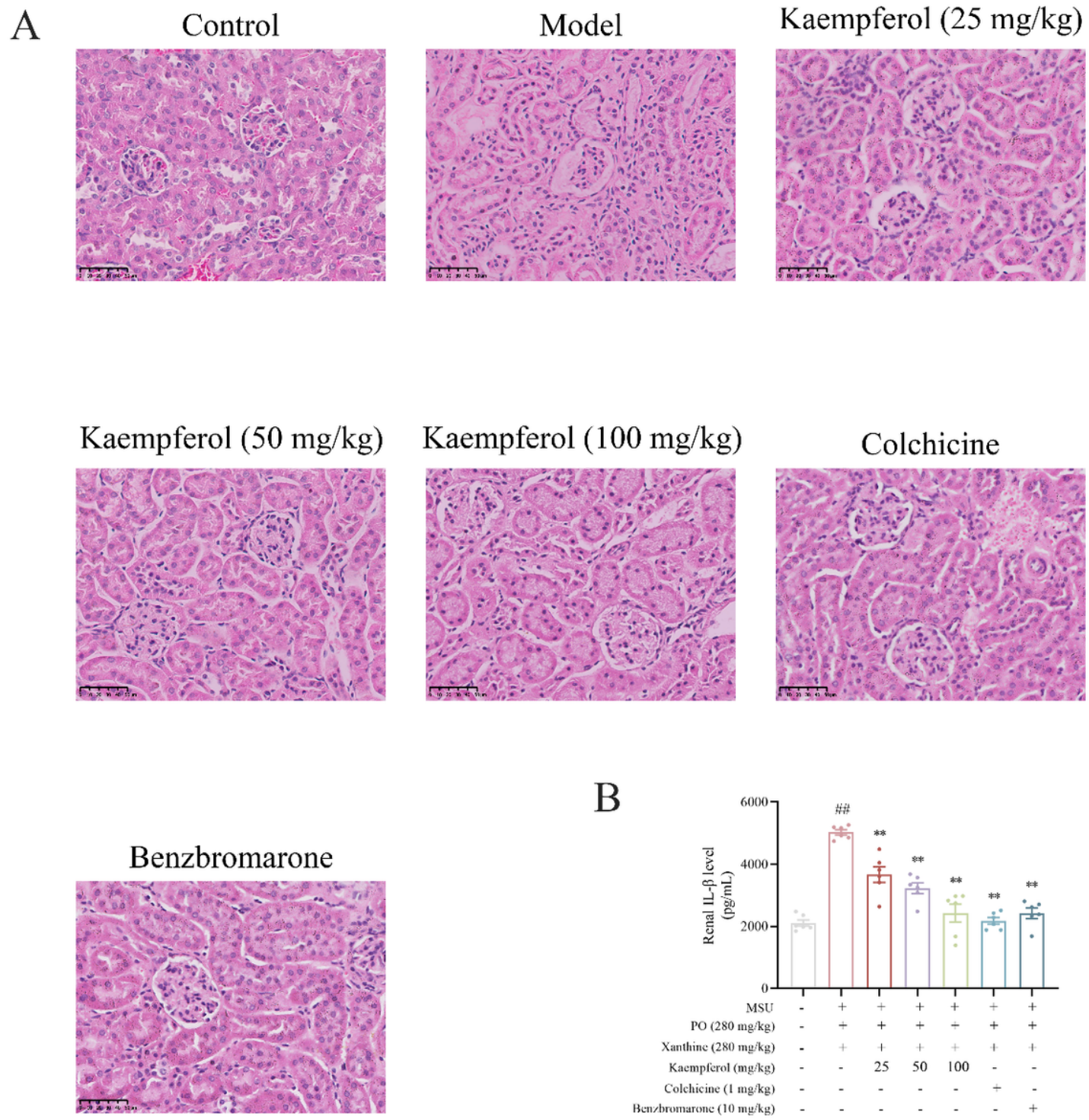

Figure 6

Representative H&E-staining in mice kidneys (**A**); Effect of kaempferol on the level of renal IL-Iβ (**B**). Data are shown as mean ± SEM (n=6). $^{\#\#}p < 0.01$ vs. control group. $^{**}p < 0.01$ vs. model group.

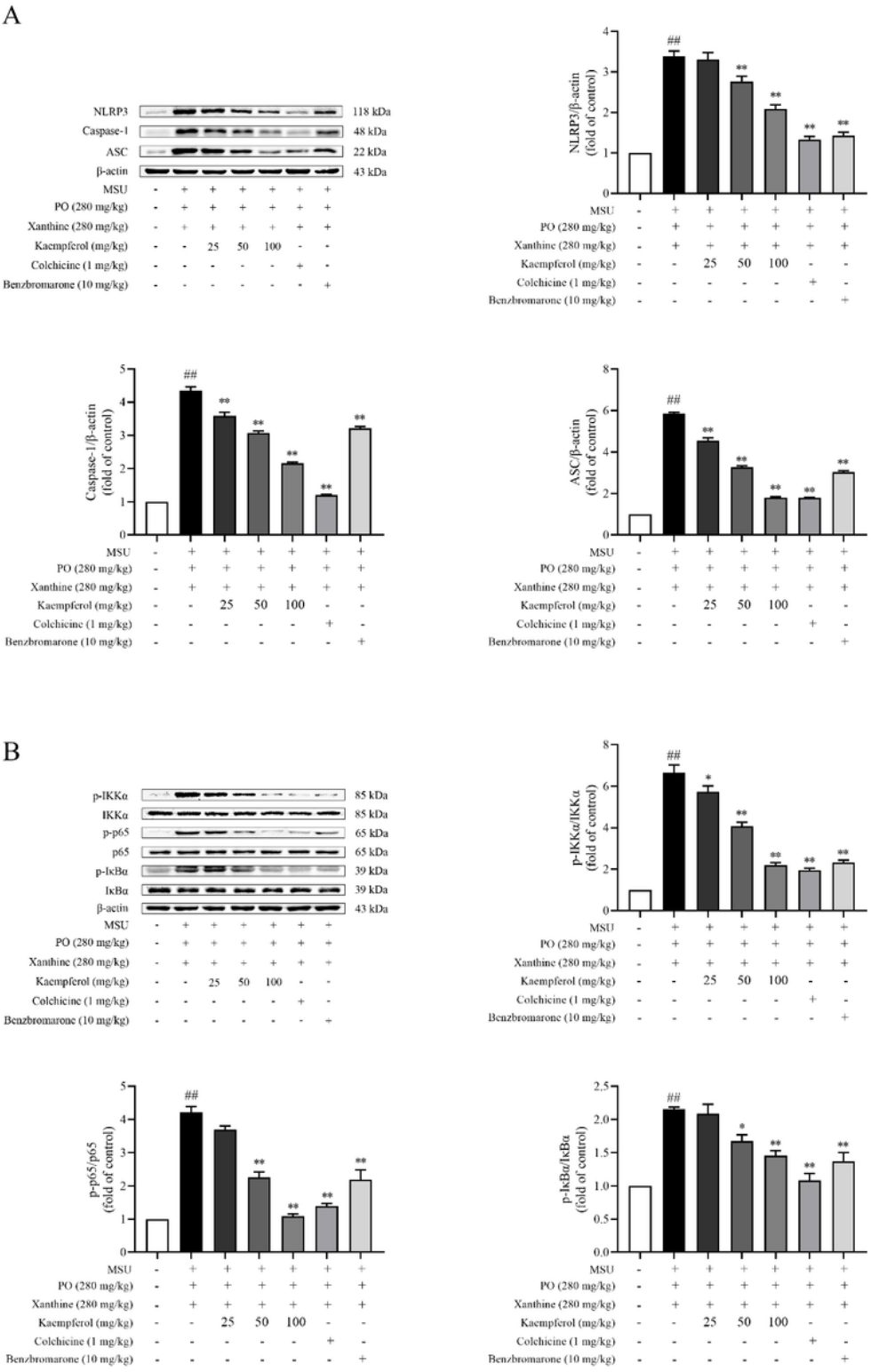

Figure 7

Effect of kaempferol on the protein expressions of NLRP3 inflammasome and NF-κB pathway in mice ankle joints: (**A**) The protein expressions of NLRP3 inflammasome components; (**B**) Related protein expressions of NF-κB pathway. Data are shown as mean ± SEM (n=3). $^{\#\#}p < 0.01$ vs. control group. $^{*}p < 0.05$, $^{**}p < 0.01$ vs. model group.

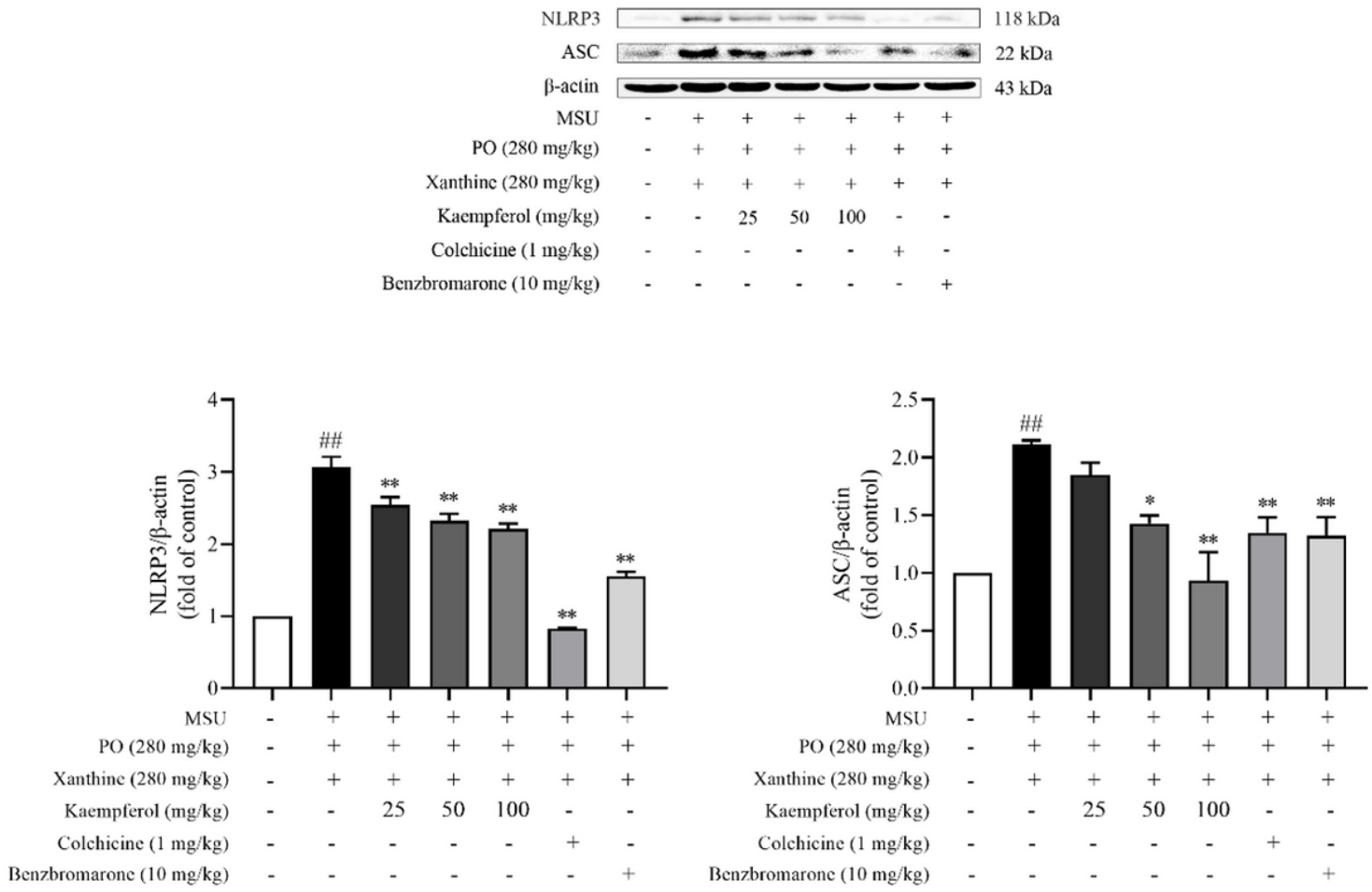

Figure 8

Effect of kaempferol on the protein expressions of NLRP3 inflammasome in mice kidneys. Data are shown as mean ± SEM (n=3). $^{\#\#}p < 0.01$ vs. control group. $^{*}p < 0.05$, $^{**}p < 0.01$ vs. model group.